



Nanoplasmonic Sensor Chip Fabricated Based on Au Nanoparticles: Effect of Graphene Oxide and Reduced Graphene Oxide

Zohreh Ayareh¹ · Mehrdad Moradi¹

Received: 4 December 2021 / Accepted: 22 March 2022 / Published online: 5 April 2022
© The Author(s), under exclusive licence to Springer Science+Business Media, LLC, part of Springer Nature 2022

Abstract

Nanoparticles of noble metals are well known to display unique optical properties due to the localized surface plasmon resonance (LSPR) phenomenon, making them applicable for use as transducers in various nanoplasmonic sensor configurations. In order to develop a sensor chip, Au nanoparticles (AuNPs) were decorated onto a substrate using a self-assembly monolayer method. The optimized substrate was subsequently prepared by functionalization with (3-Aminopropyl) triethoxysilane (APTES), while also being immersed into colloidal AuNPs. Using a uniform layer of graphene oxide (GO) and reduced GO (rGO), the AuNPs/GO and rGO hybrid structures were employed along with an appropriate optical setup acting as a smart sensor chip for detection of different concentrations of biomaterials. The optimum sensor chip (0.5% APTES; 12 h immersion time) resulted in a chip with 29% absorption and sharper plasmon peak. This appropriate condition remained constant after adding rGO, indicating that Glass/AuNPs/rGO chip will be suitable for sensory applications and detection of biomolecules.

Keywords Localized surface plasmon resonance · Au nanoparticles · Self-assembly monolayer · Plasmonic · Reduced graphene oxide · Raman spectroscopy

Introduction

Up to now, numerous novel materials with plasmonic properties based on graphene have been discovered, demonstrating very promising application in many fields, such as energy storage, sensing, and catalysis [1, 2]. The electrical conductivity, high refractive index, and large surface area of graphene materials attract widespread studies in the field of sensing [3]. The graphene-based sensor exhibits excellent performances such as label-free, and real-time detection manner for the detection of biomolecules, biomarkers, and gas sensing [4, 5]. Graphene oxide (GO) is one derivative of graphene which has a dynasty of oxygen-containing groups such as hydroxyl, epoxy, and carboxyl groups. Graphene oxide has been widely utilized as a biosensor material owing to its high electrochemical and chemical activity. Meanwhile, the π - π conjugated networks are broken with these oxidized groups [6]. The graphene oxide can be changed to the reduced graphene oxide (rGO) by removing

oxygen-containing groups, which presents different properties in certain respects. For example, the hydrophobic rGO tends to aggregation that cause to change its shape and the specific area, although the oxygen-containing groups increase the hydrophilicity so it makes GO more stable greatly in water solution [7]. The well-organized reduction of GO and restoration of π - π conjugated network of structure have provided advantages in electronics and optics fields [8]. In general, the sensors are arranged by depositing the GO or rGO suspension and other functional components such as novel metal nanoparticles on the substrate [9].

Plasmonic nanostructures have unique optical properties that can be represented by the optical cross-section and appropriate wide range of applications in biotechnology [10–12]. Au nanoparticles (AuNPs) have been used in the field of catalysis, optical sensor, energy storage, and light absorption [13–19], surface-enhanced Raman scattering (SERS) [20–22], and biological molecule detection based on their optical properties, electrical properties, and various extinction constants [23]. One well-known optical aspect of AuNPs is the localized surface plasmon resonance (LSPR), resulting from the interaction of the incident electromagnetic wave with plasmonic nanoparticles, which causes a collective oscillation of conduction electrons [24–27]. The

✉ Mehrdad Moradi
m.moradi@kashanu.ac.ir

¹ Institute of Nanoscience and Nanotechnology, University of Kashan, 87317 Kashan, Iran

wavelength and intensity of LSPR peak in extinction spectra are highly dependent on geometry, dimension in nanoscale, and the dielectric environment surrounding the nanoparticles [28, 29]. The appropriate method emphasized the deposition of graphene oxide and reduced graphene oxide onto the AuNPs nanoplasmonic sensor via metal–carbon bonding with a significantly uniform surface and suitable for binding biomolecules [30, 31]. The detection principle of the LSPR sensor chip is the measurement of the change in the refractive index of environment surrounding the plasmonic nanoparticles, as result can enhance the near-field intensity [32].

This beneficial characteristic allows monitoring of surface states and analysis of intermolecular interactions. Self-assembly monolayer is molecular layer and it has an appropriate performance which is widely used for the spontaneous arrangement of nanoparticles on the surface of the substrate. Self-assembly monolayer has been fabricated with coupling agents such as thiol-terminated, amine-terminated, alkyl-terminated, and phenyl-terminated silanes in which coupling agents are attach on various substrates through their terminal groups and adsorb metal nanoparticles on the surface of the substrate [33]. Among the coupling agents, (3-Aminopropyl) triethoxysilane (APTES) is the popular coupling agent that has been used for surface functionalization. The silanization process takes place with three hydrolysable groups APTES which are attach to hydroxyl groups on the glass substrate surface, therefore another group is the amine (NH_2) from the amino propyl groups that adsorb metal nanoparticles on the glass substrate [34]. Thus, the functionalization of the substrate with NH_2 -terminated on any substrate is exceptionally important for extra surface modification. Theoretical and experimental methods have indicated that hybrid structures combined with noble metals and graphene derivatives (GO and rGO) can cause an increase in the sensitivity of nanoplasmonic sensors. In point of fact, the transmission of surface plasmons has been altered and improved the intensity of the evanescent field at the interface by graphene-based structures. On this basis, GO/Au nanorods hybrid [35], TiO_2 -AgNPs-GO nanocomposite [36], and Au NPs/GO composite [37] have also been utilized for this purpose. These research studies reveal that AuNPs/rGO hybrid nanostructure can be utilized as appropriate substrate for increasing Raman signals of biomolecules and enhancing LSPR peak shift due to refractive index change of capture-analyte conjugation [38].

In this paper, we thus established a self-assembly monolayer process to deposit of Au nanoparticles on a transparent glass substrate as a single layer, using the functionalization of the substrate with NH_2 -terminated with 0.1, 0.5, 1, 2, and 5% APTES solution. A uniform distribution of GO and rGO was decorated on AuNPs thin film for placing chip in the optical setup to simply fabricate a nanoplasmonic sensor chip. The optimized substrate was subsequently prepared by functionalization with an ideal concentration of 0.5%

APTES, while also being immersed into colloidal AuNPs 12 h. The GO and rGO are very promising for connecting to AuNPs, and binding biomolecules.

Experimental

Gold (III) chloride trihydrate ($\text{HAuCl}_4 \cdot 3\text{H}_2\text{O}$, $\geq 99.9\%$), Trisodium citrate dihydrate ($\text{Na}_3\text{C}_6\text{H}_5\text{O}_7$, $\geq 99\%$), (3-Aminopropyl) triethoxysilane (APTES, $\geq 97\%$), Hydrochloric acid (HCl, 37%), Ethanol (99%), Methanol (MeOH, 98%), Sulfuric acid (H_2SO_4 , 98%) were purchased from Merck. Ultrapure deionized water with a resistivity of $18.2 \text{ M}\Omega\text{-cm}$ was used. The suspension of GO sheets of the modified Hummers with $2.7\text{--}6.8 \mu\text{m}$ was purchased from Namago Co. (Tehran, Iran).

Preparation of Citrate-stabilized Au Nanoparticles

Small AuNPs with a mean diameter of 10–15 nm were synthesized using the Turkevich method [39] as previously reported [40]. Citrate-stabilized Au nanoparticles were prepared in DI water via reduction of HAuCl_4 with trisodium citrate. First, a 50 ml aqueous solution of 1 mM HAuCl_4 was heated in a beaker to boil. 5 ml of 0.5 mM trisodium citrate solution was added to the HAuCl_4 solution and homogenized by gentle stirring. The mixed solution was then heated for an additional 10 min under vigorous stirring. The color of the solution immediately changed from pale yellow to red, indicating the formation of AuNPs. The reduction of Au ions and capping of resulting nanoparticles both occurred by citrate ions. Finally, the heating was stopped, and the solution of Au nanoparticles was stirred and kept in an ice bath to reach room temperature.

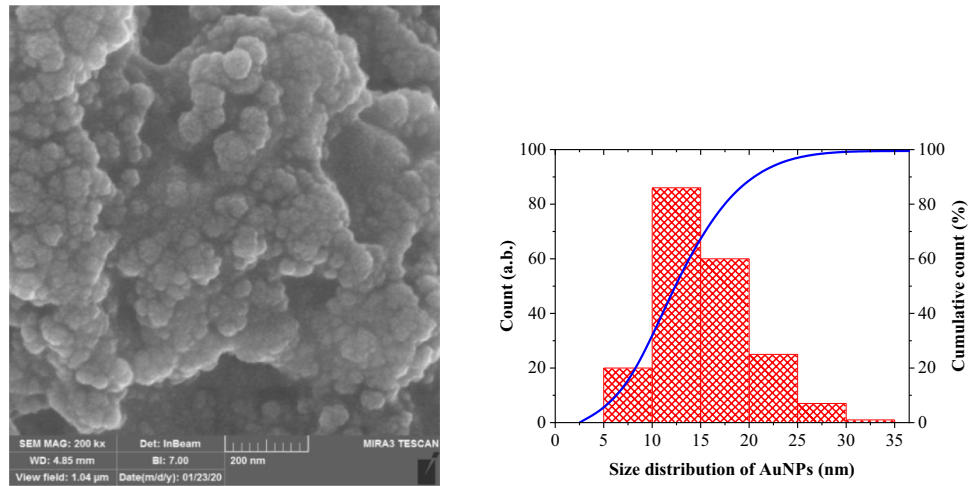
Synthesis of Graphene Oxide Derivatives

There are several ways to reduce graphene oxide, including chemical, thermal, hydrothermal, and electrochemical techniques, and chemical methods were used for the reduction of GO and change to rGO [41]. The surface composition in the method of chemically reduced graphene oxides is due to the use of different masses of hydrazine hydrate, sodium borohydride (NaBH_4), and this surface composition affect the electron transfer properties [42].

Chemical Reduced GO

Initially, 20 mg/ml of graphene oxide suspension in DI water was sonicated for 1 h to disperse the suspension. The chemical reaction was performed at 90°C . 0.16 g of NaBH_4 was added to the above mixture under continuous stirring. The reaction ended after 48 h. Finally, the product was washed with DI water until the pH reached neutral and dried in an oven at 65°C [43].

Fig. 1 The FESEM image of colloidal Au nanoparticles and size distribution diagram of nanoparticles



Chip Fabrication and Optimization of APTES Concentration

The nanoplasmonic sensor chip was fabricated in three steps: hydroxylation of the glass substrate (-OH), silanization of the glass substrate (-NH₂), and attachment of colloidal gold nanoparticles on the glass surface. In the first step, for hydroxylation of the microscope substrate, the glass slides were cut into 7 × 1 cm² pieces and cleaned by immersion in freshly prepared 1:1 MeOH:HCl solution for 30 min, after that immersed in H₂SO₄ for 30 min, followed by rinsing in distilled water and ethanol in an ultrasonic bath, and drying under a stream of N₂. After cleaning, for silanization process, the hydroxyl-functionalized slides were immersed in 0.1, 0.5, 1, 2, and 5% APTES solution in ethanol for 1 h, rinsed with ethanol, and dried with N₂ gas.

In the third step, AuNPs immobilization was achieved by immersing the silanized slides in a colloidal citrate-stabilized

AuNPs at various times. By immersion in the colloidal gold nanoparticle solution for 1 and 12 h, two types of nanoplasmonic sensor chips were prepared, and entitled type 1 and type 2, respectively. The sensor chips were then rinsed with water to remove the unbinding AuNPs. A uniform layer of GO and rGO sheets was dip-coated on the AuNPs thin films. At this step, the AuNPs thin films were first immersed in a colloidal solution of GO or rGO for 1 min and drawn upward at a constant rate of 187.5 mm min⁻¹ for 3 min.

Characterization

The nanoplasmonic sensor chip includes citrate-stabilized AuNPs immobilized on a glass substrate modified with the organic adhesion layer. The morphology of Au nanoparticles and thin films was visualized by a field emission scanning electron microscope (FESEM) to study the uniformity of the AuNPs monolayer (TESCAN-MIRA3). The UV–Vis

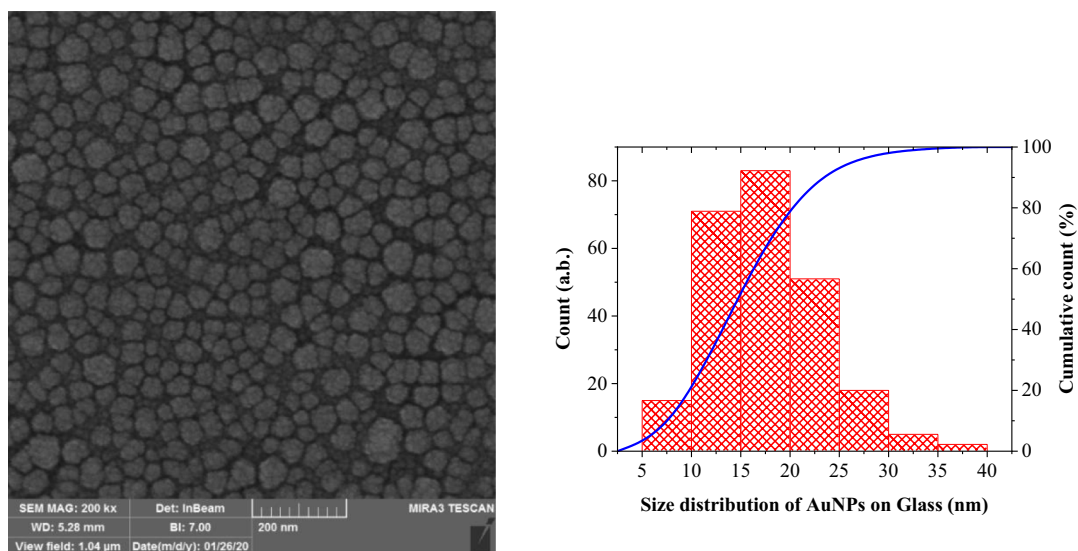


Fig. 2 The FESEM image of Au nanoparticles on glass surface after annealing and size distribution diagram of nanoparticles

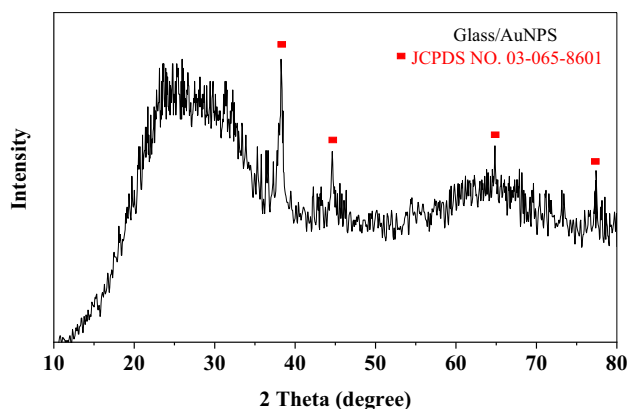


Fig. 3 X-ray diffraction pattern of AuNPs thin film on glass substrate

spectrum was measured for plasmon absorption analysis (Spectronix Ar 2015). XRD pattern was registered by employing an X-ray diffractogram (Philips) with copper K_{α} irradiation ($\lambda = 15.4$ nm). FT-IR spectrum was measured by the Shimadzu Varian 4300 spectrophotometer in the range of 400–4000 cm^{-1} . Raman spectra were recorded using Lab Ram HR Raman microscope (Horiba) with $50\times/0.50\text{NA}$ objective, and a source excitation was 532 nm of green laser.

Results and Discussion

Morphological Study

Figure 1 shows that the colloidal AuNPs are close to spherical Au nanoparticles with citrate stabilized. After assembly of AuNPs monolayer on the substrate, annealing at temperatures close to T_g (the glass transition temperature is the temperature at which the molecular structure shows molecular

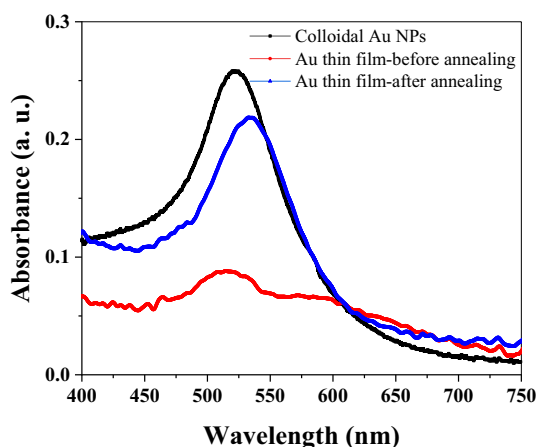


Fig. 4 The absorbance of colloidal AuNPs, the AuNPs on glass surface before and after annealing

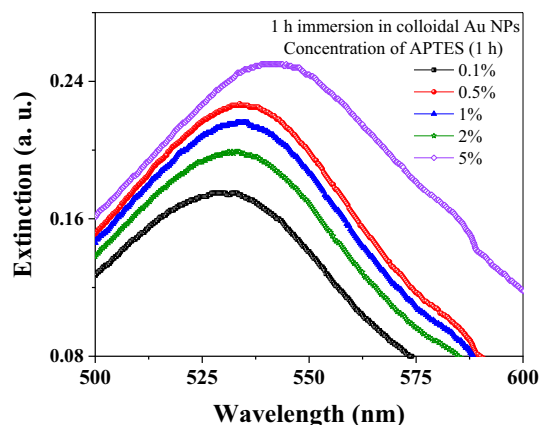


Fig. 5 The extinction of nanoplasmonic sensor chips (type 1), 1 h in APTES with different concentration 0.1, 0.5, 1, 2, 5% and 1 h immersion in colloidal AuNPs

mobility) of the AuNPs thin films (557 °C) results in significant enhancement of the adhesion between the AuNPs and the substrate. Therefore, sensor chips were annealed at 550 °C at a rate of 5 °C/min and stayed at this temperature for 4 h. The FESEM image illustrates the size distribution of 10–15 nm for the nanoparticles (Fig. 1). After the annealing process, the AuNPs were deposited uniformly and densely on the substrate. Because of the aggregation of nanoparticles, the size distribution increased to about 15–20 nm (Fig. 2).

Optical Properties and Characterization of GNPs

Figure 3 reveals the XRD pattern of metallic Au nanoparticles on the glass substrate. All diffraction peaks corresponding to face-centered cubic (fcc) (111), (200), (220), and (311) crystalline planes were well-matched with the

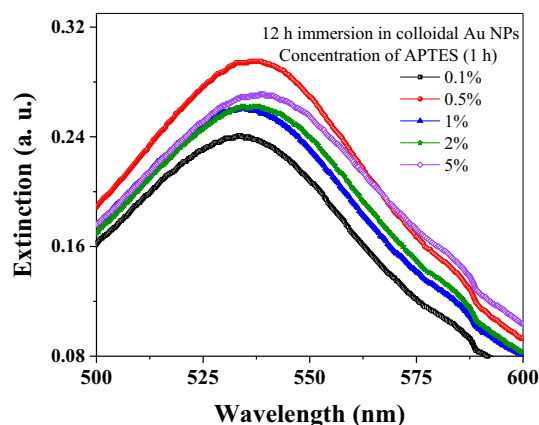


Fig. 6 The extinction of nanoplasmonic sensor chips (type 2), 1 h in APTES with different concentration 0.1, 0.5, 1, 2, 5% and 12 h immersion in colloidal AuNPs

Table 1 The extinction wavelength, FWHM and intensity of nanoplasmonic sensor chips (according to Figs. 5 and 6)

APTES (1 h)	1 h immersion in colloidal AuNPs(type 1)					12 h immersion in colloidal AuNPs(type 2)				
	0.1%	0.5%	1%	2%	5%	0.1%	0.5%	1%	2%	5%
Wavelength (nm)	530	535	534	533	543	533	537	534	537	539
Intensity of extinction (a. b.)	0.175	0.226	0.216	0.199	0.25	0.241	0.295	0.261	0.262	0.271
FWHM (nm)	55.62	55.36	55.47	55.93	60.27	55.92	55.42	56.56	57.74	62.75

JCPDS No. 03–065-8601 of Au metal. The XRD pattern of Au with the background of glass pattern confirms the distance between Au nanoparticles on the surface. The extinction spectrum of nanoplasmonic sensor chips before and after annealing was characterized by UV–Vis spectroscopy and shown in Fig. 4. The UV–Vis spectrum of colloidal AuNPs exhibits a plasmon resonance peak at 522 nm. Annealing of AuNPs thin films leads to an enhancement in the extinction intensity and 10 nm LSPR red-shift. As the nanoparticle size increases, not only does the adsorption rate increase but also the position and width of the LSPR shift.

Nanoplasmonic sensor chips were performed to optimize the immobilization of amine functional groups on the glass substrate with different concentrations and immersion time of APTES, which attends as a linking molecule between the glass and the AuNPs. The self-assembly takes place through electrostatic interaction between the positively charged amine group and negatively charged AuNPs.

Figures 5 and 6 depict the surface plasmon peak changes of the sensor chips to determine the optimal APTES concentration and immersion time in colloidal AuNPs. As shown in Fig. 5, increasing the APTES concentration not only enhances the extinction intensity of the sensor chip but also causes an LSPR red-shift. However, this treatment has not been followed in Fig. 6. Based on the results shown in Table 1, 0.5% APTES and 12 h immersion time in AuNPs were selected as the optimal condition for the sensor chip. Since this chip demonstrates the highest extinction intensity and sharp plasmon peak (smaller FWHM), it is highly sensitive for detection of biomolecules.

Due to the synergistic effects, novel metal/graphene nanostructure hybrids exhibit advanced performance in biosensors compared to NPs and graphene derivatives taken independently. Hence, attempts have been focused on the decoration of GO/rGO surfaces with AuNPs, which have applications in various fields such as catalysts, biosensors, surface-enhanced Raman scattering (SERS), and surface-enhanced infrared absorption (SEIRA). Recently, the coating of GO and rGO has improved the sensitivity of SERS substrates and LSPR sensors by absorbing more capture probe from biomolecules. We adopted the dip-coating method, one of the simplest methods, to coat GO and rGO on the surface of AuNPs thin films. In continuance, we compared two types of nanoplasmonic sensor chips, comprising either GO or rGO.

Figure 7 shows the FTIR spectra of GO and rGO in which the GO spectrum contains the absorption bands corresponding to –OH stretch at 3428 cm⁻¹, the C=O carbonyl stretching vibrations at 1602 cm⁻¹, the C–OH stretching at 1384 cm⁻¹, and the epoxy C–O stretching at 1014 cm⁻¹. The spectrum of rGO shows peaks at 3428 cm⁻¹, corresponding to –OH stretch, while the bands of carboxyl, epoxy, and carbonyl were removed after the reduction [44, 45].

Based on the outcomes, the AuNPs thin film for depositing GO and rGO was selected with 0.5% APTES and 12 h immersion in colloidal AuNPs as the optimal condition for the sensor chip. The GO and rGO layers were used owing to their inherent properties of binding the biomolecules and increasing the interaction light with structure [46, 47]. The morphology of sensor chips (AuNPs/GO and AuNPs/rGO) was observed using SEM. As shown in Fig. 8A, the GO

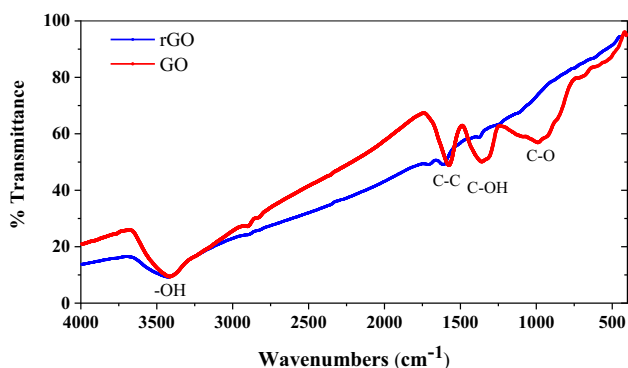


Fig. 7 FT-IR spectra of GO and rGO sheets

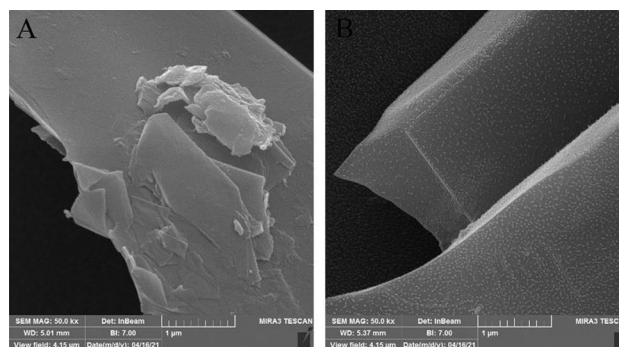


Fig. 8 The FESEM image of LSPR chip of A AuNPs/rGO sheets, and B AuNPs/GO sheets

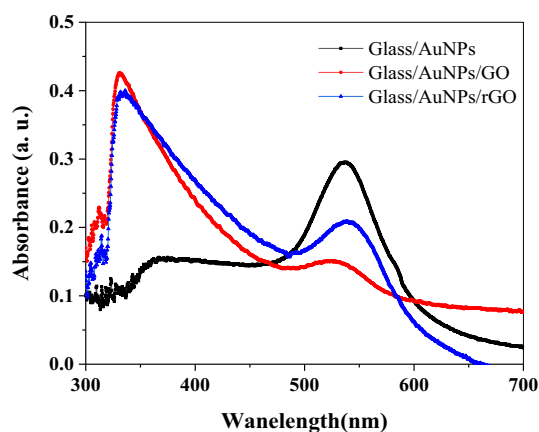


Fig. 9 The absorbance spectra of Glass/AuNPs, sensor chip of AuNPs/GO, and sensor chip of AuNPs/rGO

sheets were recognized in the SEM image. Similarly, the SEM images of AuNPs/GO and AuNPs/rGO are presented, demonstrating the uniform distribution of paper-like GO and rGO sheets on AuNPs thin film. In Fig. 8B, it was found that rGO with sheet morphology has an appropriate length and interlayer spacing.

According to Fig. 9, all absorption peaks associated with the GO and rGO sheets are in the visible range of 400–900 nm, which is the wavelength range of AuNPs LSPR [48]. Detection of the local index of refraction using UV–Visible spectrum corresponding to sharp plasmon peaks for high sensitivity. In this case, sensor chip of AuNPs/rGO has sharp plasmon peaks rather than other chips, and red-shift confirms the binding of AuNPs and rGO.

Figure 10 shows the Raman spectra of the AuNPs/GO and the AuNPs/rGO sensor chips displaying the G band (1593 cm^{-1}) for vibration mode in-plane of sp^2 carbon

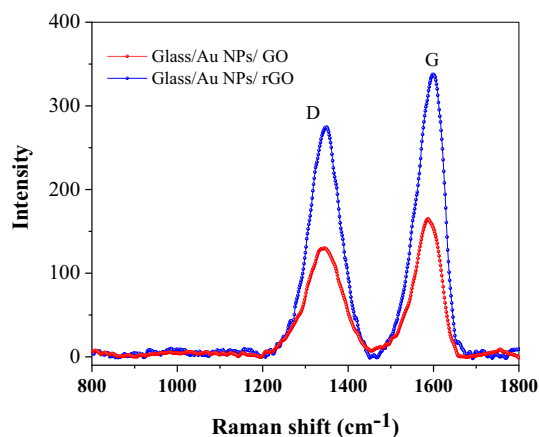


Fig. 10 The Raman spectra of sensor chip of AuNPs/GO and sensor chip of AuNPs/rGO

domains and D band (1347 cm^{-1}) associated with structural defects indicating the reduction in the size of sp^2 domains and increasing of out-plane of sp^3 domains. The I_D/I_G ratio can be described as the number of defects of GO and rGO in the sensor chips. For the sensor chip of AuNPs/GO, the value of I_D/I_G is equal to 0.78, while for AuNPs/rGO it increases to 0.81. An increase in I_D/I_G shows that partial reduction has increased structural defects in the GO carbon plane [49]. Significant differences in intensity peaks can confirm the widespread coupling of AuNPs with rGO, which increases the light interaction in the advanced SERS configuration. Consequently, the fabricated AuNPs/rGO hybrid structure can serve as a nanoplasmonic sensor chip to detect refractive index change of receptor-analyte conjugation, being a more capable SERS substrate for the detection of biomolecules. This hybrid structure will have great potential for the detection of capture probe-target analyte conjugation (aptamers, proteins and antibodies as capture probes), and eventually biomolecules such as DNA, protein and any antigens [50].

Conclusions

The AuNPs thin films were prepared by electrostatic binding of citrate-stabilized NPs on amino silane-terminated glass substrates. Those were fabricated with different concentrations of APTES and immersion time in colloidal AuNPs to enhance the sensitivity of the nanoplasmonic sensor chip. After annealing of the AuNPs thin films at 550°C , the AuNPs were deposited most uniformly and densely. The extinction of the sensor chip demonstrated that the best condition in the fabrication of sensor chip was 0.5% APTES and 12 h immersion time in AuNPs (type 2). The GO and rGO were found to be very promising for connecting to AuNPs and binding biomolecules, so that AuNPs/GO and AuNPs/rGO hybrid nanostructures could be employed as efficient biosensor chips. By evaluating the two chips, it is found that the Glass/AuNPs/rGO as a nanoplasmonic sensor chip will be suitable for sensory applications, adsorbing capture probe-target analyte conjugation, and detecting biomolecules.

Author Contribution Zohreh Ayareh: Investigation, Visualization, Writing – original draft. Mehrdad Moradi: Supervision, Conceptualization, Resources.

Funding The authors gratefully acknowledge the financial support of this study from the University of Kashan by Grant No. 1093744/1.

Data Availability All data that support the findings of this study are available from the corresponding author upon reasonable request.

Code availability Not applicable.

Declarations

Ethics Approval and Consent to Participate Informed consent was obtained from all individual participants included in the study.

Consent for Publication All the authors agree to publish these papers.

Conflict of Interest The authors declare no competing interests.

References

- Li M, Tang Z, Leng M, Xue J (2014) Flexible solid state super capacitor based on graphene-based hybrid films. *Adv Funct Mater* 24:7495–7502
- Kakaei K, Balavandi A (2016) Synthesis of halogen-doped reduced graphene oxide nanosheets as highly efficient metal free electrocatalyst for oxygen reduction reaction. *J Colloid Interf Sci* 463:46–54
- Tiwari JN, Vij V, Kemp KC, Kim KS (2016) Engineered carbon-nanomaterial-based electrochemical sensors for biomolecules. *ACS Nano* 10:46–80
- Wang T, Huang D, Yang Z, Xu SS, He GL, Li XL, Hu NT, Yin GL, He DN, Zhang LYA (2016) Review on graphene-based gas/vapor sensors with unique properties and potential applications. *Nano-Micro Lett* 8:95–119
- Yang YJ, Li WK (2014) Gold nanoparticles/graphene oxide composite for electrochemical sensing of hydroxylamine and hydrogen peroxide. *Fuller Nanotub Carbon Nanostruct* 26:195–204
- Zhao J, Pei S, Ren W, Gao L, Cheng HM (2010) Efficient preparation of large-area graphene oxide sheets for transparent conductive films. *ACS Nano* 4:5245–5252
- Stankovich S, Piner RD, Chen X, Wu N, Nguyen ST, Ruoff RS (2006) Stable aqueous dispersions of graphitic nanoplatelets via the reduction of exfoliated graphite oxide in the presence of poly (sodium 4-styrenesulfonate). *J Mater Chem* 16:155–158
- Lin T, Chen I, Liu F, Yang C, Bi H, Xu F, Huang F (2015) Nitrogen doped mesoporous carbon of extraordinary capacitance for electrochemical energy storage. *Science* 350:1508–1513
- Wang D, Li W, Zhang Q et al (2021) High-performance tapered fiber surface plasmon resonance sensor based on the graphene/Ag/TiO₂ layer. *Plasmonics* 16:2291–2303
- Xu T, Geng Z (2021) Strategies to improve performances of LSPR biosensing: structure, materials, and interface modification. *Biosens Bioelectron* 174:112850
- Li Z, Butun S, Aydin K (2014) Touching gold nanoparticle chain based plasmonic antenna arrays and optical metamaterials. *ACS Photonics* 1(3):228–234
- Baciu CL, Becker J, Janshoff A, Sönnichsen C (2008) Protein-membrane interaction probed by single plasmonic nanoparticles. *Nano Letter* 8(6):1724–1728
- Wang BX, He Y, Lou P, Xing W (2020) Design of a dual-band terahertz metamaterial absorber using two identical square patches for sensing application. *Nanoscale Adv* 2(2):763–769
- Wang BX, He Y, Lou P, Zhu H (2021) Multi-band terahertz superabsorbers based on perforated square-patch Metamaterials. *Nanoscale Adv* 3(2):455–462
- Wang BX, Xu Wei Wu Y, Yang Z, Lai S, Lu L (2022) Realization of a multi-band terahertz metamaterial absorber using two identical split rings having opposite opening directions connected by a rectangular patch. *Nanoscale Adv* 4(5):1359–1367
- Wang BX, Wu Y, Xu W, Yang Z, Lu L, Pi F (2022) Quad-band terahertz metamaterial absorber enabled by an asymmetric I-type resonator formed from three metallic strips for sensing application. *Sens Diagn* 1(1):169–176
- Wang BX, Tang C, Niu Q et al (2019) Design of narrow discrete distances of dual-/triple-band terahertz metamaterial absorbers. *Nanoscale Res Lett* 14:64
- Moradi M, Ayareh Z, Mahmoodi S (2019) Magneto-plasmonic biosensing platform for detection of glucose concentration. *Optik* 178:765–773
- Mahmoodi S, Moradi M (2018) carbon nanotube assisted enhancement of the magneto-optical Kerr signal in nickel thin films. *J Electron Mater* 47:7069–7074
- Kasztelan M, Słoniewska A, Gorzkowski M, Lewera A, Pałys B, Zoladek S (2021) Ammonia modified graphene oxide-gold nanoparticles composite as a substrate for surface enhanced Raman spectroscopy. *Appl Surf Sci* 554:149060
- Santhoshkumar S, Murugan E (2021) Rationally designed SERS AgNPs/GO/g-CN nanohybrids to detect methylene blue and Hg²⁺ ions in aqueous solution. *Appl Surf Sci* 553:149544
- Jimenez-Vara PB, Johnny J, Novoa-de Leon IC, Guerrero-Bermea C, Garcia-Gutierrez DF, Garcia-Gutierrez DI Chavez-Guerrero L, Sepulveda-Guzman S (2020) Hybrid films of reduced graphene oxide modified with gold nanorods and its study as surface-enhanced Raman spectroscopy platform. *Mater Lett* 265:127405
- Zohora N, Kumar D, Yazdani M, Rotello VM, Ramanathan R, Bansal V (2017) Rapid colorimetric detection of mercury using biosynthesized gold nanoparticles. *Colloid Interface Sci* 532:451–457
- Sepúlveda B, Angelomé PC, Lechuga LM, Liz-Marzán LM (2009) LSPR-based nanobiosensors. *Nano Today* 4:244–251
- Esmailzadeh B, Moradi M (2018) Enhancement of Kerr signal in Co thin films incorporating Ag nanoparticles surrounded by TiO₂. *J Supercond Nov Magn* 31:1483–1488
- Guerreiro JRL, Frederiksen M, Bochenkov VE, De Freitas V, Ferreira SMG, Sutherland DS (2014) Multifunctional biosensor based on localized surface plasmon resonance for monitoring small molecule-protein interaction. *ACS Nano* 8(8):7958–7967
- Xu T, Geng Z (2020) Strategies to improve performances of LSPR biosensing: structure, materials, and interface modification. *Biosens Bioelectron* 174:112850
- Dormeny AA, Sohi PA, Kahrizi M (2020) Design and simulation of a refractive index sensor based on SPR and LSPR using gold nanostructures. *Results Phys* 16:102869
- Taghavi A, Rahbarizadeh F, Abbasian S et al (2015) Label-free LSPR prostate-specific antigen immune-sensor based on GLAD-fabricated silver nano-columns. *Plasmonics* 15:753–760
- Prabowo BA, Purwidyantri A, Liu B, Lai HC, Liu KC (2021) Gold nanoparticle-assisted plasmonic enhancement for DNA detection on a graphene-based portable surface plasmon resonance sensor. *Nanotechnol* 32(9):095503
- Barghouti ME, Akjouj A, Mir A (2018) Effect of graphene layer on the localized surface plasmon resonance (LSPR) and the sensitivity in periodic nanostructure. *Photo Nano Fund Appl* 31:107–114
- Willetts KA, Duyne RPV (2007) Localized surface plasmon resonance spectroscopy and sensing. *Annu Rev Phys Chem* 58:267–297
- Kyaw HH, Al-Harathi SH, Sellai A, Dutta J (2015) Self-organization of gold nanoparticles on silanated surfaces. *Beilstein J Nanotechnol* 6:2345–2353
- Terracciano M, Rea I, Politi J, De Stefano K (2013) Optical characterization of amino silane-modified silicon dioxide surface for biosensing. *J Eur Opt Soc* 8:13075
- Li JJ, An HQ, Zhu J, Zhao JW (2015) Improve the surface enhanced Raman scattering of gold nanorods decorated graphene oxide: the effect of CTAB on the electronic transition. *Appl Surf Sci* 347:856–860
- Zhang M, Sun H, Chen X et al (2021) The influences of graphene oxide (GO) and plasmonic Ag nanoparticles modification on the

- SERS sensing performance of TiO₂ nanosheet arrays. *J Alloys Compd* 864:158189
37. Kasztelan M, Słoniewska A, Gorzkowski M et al (2021) Ammonia modified graphene oxide – gold nanoparticles composite as a substrate for surface enhanced Raman spectroscopy. *Appl Surf Sci* 554:149060
 38. Oh SH, Altug H, Jin X et al (2021) Nanophotonic biosensors harnessing van der Waals materials. *Nat Commun* 12:3824
 39. Turkevich J, Stevenson PC, Hillier J (1951) A study of the nucleation and growth processes in the synthesis of colloidal gold. *Discuss Faraday Soc* 11:55–75
 40. Moradi M, Ayareh Z, Mahmoodi S (2017) Enhancement of magneto-optical Kerr response by LSPR in magneto plasmonic nanostructures for biological sensors. *J Magn Magn Mater* 444:410–415
 41. Feng J, Ye Y, Xiao M, Wu G, Ke Y (2020) Synthetic routes of the reduced graphene oxide. *Chem Pap* 74:3767–3783
 42. Tan SM, Ambrosi A, Chua CK, Pumera M (2014) Electron transfer properties of chemically reduced graphene materials with different oxygen contents. *J Mater Chem A* 2:10668–10675
 43. Báez DF, Pardo H, Laborda I, Marco JF, Yáñez C, Bollo S (2017) Reduced graphene oxides: influence of the reduction method on the electrocatalytic effect towards nucleic acid oxidation. *Nanomater* 7(7):168
 44. Yang Z, Zheng Q, Qiu H, Li J, Yang J (2015) A simple method for the reduction of graphene oxide by sodium borohydride with CaCl₂ as a catalyst. *New Carbon Mater* 30(1):41–47
 45. Goncalves G, Marques PAP, Granadeiro CM, Nogueira HIS, Singh MK, Gracio J (2009) Surface modification of graphene nanosheets with gold nanoparticles: the role of oxygen moieties at graphene surface on gold nucleation and growth. *Chem Mater* 21:4796–4802
 46. Xiong X, Chen Y, Wang H, Hu S, Luo Y, Dong J, Zhu W, Qiu W, Guan H, Lu H, Yu J, Zhang J, Chen Z (2018) Plasmonic interface modified with graphene oxide sheets over layer for sensitivity enhancement. *ACS Appl Mater Interfaces* 10(41):34916–34923
 47. Liu X, Zhao Z, Shen T, Qin Y (2019) Graphene/gold nanoparticle composite-based paper sensor for electrochemical detection of hydrogen peroxide. *Fuller Nanotub Carbon Nanostruct* 27:23–27
 48. Singh L, Zhang RB, Cheng S, Kaushik BK, Kumar S (2019) LSPR based uric acid sensor using graphene oxide and gold nanoparticles functionalized tapered fiber. *Opt Fiber Technol* 53:102043
 49. Abdelkader-Fernández VK, Melguizo M, Domingo-García M, López-Garzón FJ, Pérez-Mendoza M (2019) Hydrogen cold plasma for the effective reduction of graphene oxide. *Appl Surf Sci* 464:673–681
 50. Altug H, Oh SH, Maier SA, Homola J (2022) Advances and applications of nanophotonic biosensors. *Nat Nanotechnol* 17:5–16

Publisher's Note Springer Nature remains neutral with regard to jurisdictional claims in published maps and institutional affiliations.